

M. Maekawa  
M. Kondo

## Effects of affinity and aggregation on parallel diffusion of tri-sulfonated azo compounds into water-swollen cellulose membranes

Received: 7 February 1996  
Accepted: 14 May 1996

Dr. M. Maekawa (✉) · M. Kondo  
Division of Life Science and Human  
Technology  
Nara Women's University  
Nara 630, Japan

**Abstract** Adsorption and diffusion of tri-sulfonated azo dyes, C.I. Acid Red 18 and C.I. Acid Red 27 onto water-swollen cellulose membrane has been studied at 25 °C. Affinities of these dyes onto cellulose were evaluated by the coefficients of Freundlich equation. Diffusion behavior of these dyes was analyzed on the basis of a parallel transport theory by surface and pore diffusion. The results could be described by the parallel diffusion model provided that adsorption was

stimulated by addition of NaCl. The surface diffusivities for the parallel diffusion model were correlated by the affinity of the dyes, on the other hand, the pore diffusivities for the model were affected by aggregation of the dye depending on its structure and NaCl concentration.

**Key words** Anionic dye – aggregation – affinity – cellulose membrane – parallel transport theory

### Introduction

Adsorption and diffusion behavior of substances onto porous materials like activated carbon or polymer membrane has been of interest in various fields. Many studies had been carried out on adsorption and diffusion behavior of dyes onto polymeric materials [1–4]. We also have studied adsorption and diffusion behavior of various anionic dyes into a water-swollen cellulose membrane and analyzed this on the basis of a parallel transport theory in our previous papers [5–10]. It was revealed that 1) the diffusion can be described by parallel diffusion of surface and pore diffusion, where the surface diffusion means the diffusion of dyes in the adsorbed state on the inner surface of pore wall of cellulose membrane and the pore diffusion means the diffusion of dyes in the liquid phase in the membrane; 2) diffusion of the dyes with a certain affinity to the substrate is mainly controlled by surface diffusion rather than pore diffusion; 3) the surface diffusivity of the parallel diffusion model correlates well with the molecular

weight of the dyes, on the other hand, the pore diffusivity of the parallel diffusion model was affected by aggregation of dye molecules.

In the present paper, we study the adsorption and diffusion behavior of two tri-sulfonated azo dyes with a low affinity. Then, we discuss how their affinity and aggregation affect the surface and pore diffusivities of the parallel diffusion model.

### Experimental

#### Materials

Tri-sulfonated dyes, C.I. Acid Red 18 and C.I. Acid Red 27 (M.W. = 604.48, Tokyo Kasei Co.) were purified by Robinson Mills' method [11]. The structural formulas are shown in Fig. 1. The cellulose membrane (cellophane film) supplied by Rengo Co. was soaked in boiled deionized water for 3 h (30 min × 6 times) and then washed with

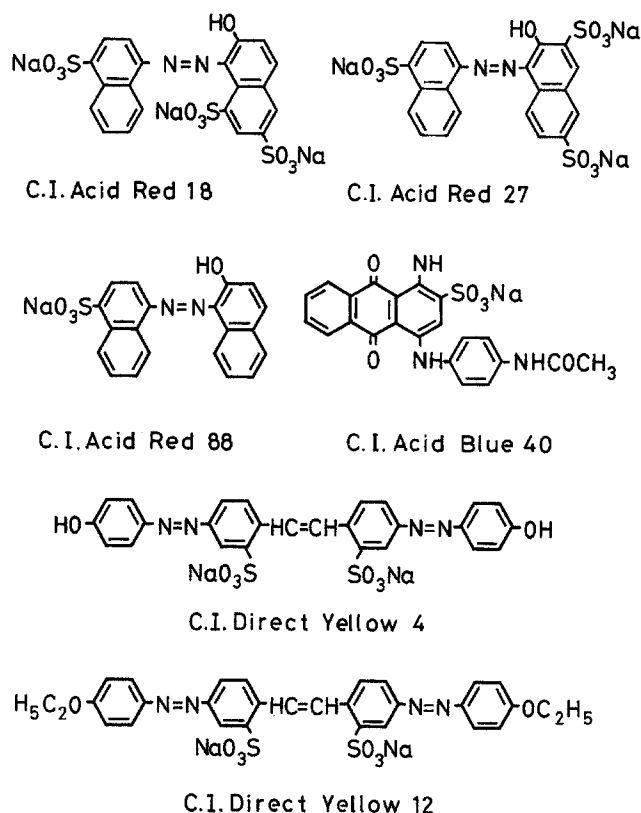


Fig. 1 The structural formulae of the dyes

deionized distilled water. The experimental thickness ( $l$ ) measured by a membrane-thickness meter (Kohbunshi keiki Co., Ltd), void fraction ( $\varepsilon_p$ ) and the volume ( $V$ ) measured by the pycnometric method (6) of the water-swollen membrane per unit dry cellulose were 38.6  $\mu\text{m}$ , 0.733 and 2.38  $\text{dm}^3/\text{kg}$ , respectively. Sodium chloride (guaranteed reagent) was obtained from Nakarai tesque and used after drying.

#### Diffusion of the dye – adsorption isotherms

Equilibrium isotherms for adsorption of the dyes on the cellulose membrane were measured by the batch method. Equilibrium was attained in 3 h.

Rate of dyeing (uptake) curves and concentration-distance profiles were measured by using an ultrafiltration type cell with water jacket. The membrane was placed on a plastic plate at the bottom of the cell to establish non-steady-state diffusion as described elsewhere [5–7]. Uptake curves were generated by the integral step method using one sheet of the membrane. The concentration-distance profiles were measured by placing a stack of ten membranes together during the experiments and sepa-

rating them for concentration analysis. The amount of the dye adsorbed over a given period was determined by desorption of the dye from the membrane with 25% aqueous pyridine and measuring its concentration using a Hitachi U-3200 spectrophotometer with 25% pyridine as a reference. Experiments were carried out at 25 °C.

#### Theoretical

In the theoretical development of the diffusion equations, it is assumed that 1) surface and pore diffusion occur in parallel within a cellulose membrane, 2) pore and surface diffusivities are constant during the adsorption process, 3) the pore diameter and the void fraction of the membrane are constant during the adsorption process, 4) the concentration of the dye anions in the pores is in local equilibrium with the concentration of adsorbed dye anions on the surface of the pore wall, and 5) the diffusion of sodium chloride is complete before significant diffusion of the dye molecules.

These assumptions lead to the following mass balance equation:

$$\varepsilon_p \frac{\partial C}{\partial t} + \frac{\partial q}{\partial t} = \varepsilon_p D_p \frac{\partial^2 C}{\partial z^2} + D_s \frac{\partial^2 q}{\partial z^2}, \quad (1)$$

where  $C$  and  $q$  are the concentrations of the dye in the pores and on the surface of the pore wall, respectively ( $\text{mol}/\text{m}^3$ ).  $t(\text{s})$  and  $z(\text{m})$  represent time and distance through membrane.  $\varepsilon_p$  is the void fraction of the membrane.  $D_p$  and  $D_s$  represent the pore and surface diffusivities, respectively ( $\text{m}^2/\text{s}$ ). Using the dimensionless variables defined in Eq. (2), Eq. (1) can be transformed to give Eq. (3).

$$\tau_p = \frac{D_p t}{l^2}, \quad \rho = \frac{z}{l}, \quad x = \frac{C}{C_0},$$

$$y = \frac{q}{q_0}, \quad \alpha = \frac{q_0}{\varepsilon_p C_0}, \quad \beta = \alpha \frac{D_s}{D_p} \quad (2)$$

$$\frac{\partial x}{\partial \tau_p} + \alpha \frac{\partial y}{\partial \tau_p} = \frac{\partial^2 x}{\partial \rho^2} + \beta \frac{\partial^2 y}{\partial \rho^2}, \quad (3)$$

where  $C_0$  is dye concentration in the bulk solution and  $q_0$  is adsorbed concentration of dye in equilibrium with  $C_0$  ( $\text{mol}/\text{m}^3$ ). There are two limiting cases:  $\beta = 0$  (pore diffusion control) and  $\beta = \infty$  (surface diffusion control). However, Eq. (3) cannot be solved for  $\beta = \infty$ , and hence Eq. (1) is transformed to Eq. (4):

$$\frac{\partial x}{\partial \tau_s} + \alpha \frac{\partial y}{\partial \tau_s} = \alpha \frac{\partial^2 y}{\partial \rho^2}, \quad (\text{surface diffusion control}) \quad (4)$$

where  $\tau_s = D_s t/l^2$ . The relation between  $x$  and  $y$  is calculated according to the equilibrium isotherm (fourth

assumption). Applying the Freundlich isotherm defined by Eq. (5), we transformed Eqs. (3) and (4) into Eqs. (6) and (7), respectively.

$$y = x^\gamma \quad (5)$$

$$\left[ \alpha + \frac{1}{\gamma} y^{(1-\gamma)/\gamma} \right] \frac{\partial y}{\partial \tau_p} = \frac{1}{\gamma} \frac{\partial}{\partial \rho} \left[ y^{(1-\gamma)/\gamma} \frac{\partial y}{\partial \rho} \right] + \beta \frac{\partial^2 y}{\partial \rho^2} \quad (6)$$

$$\left[ \alpha + \frac{1}{\gamma} y^{(1-\gamma)/\gamma} \right] \frac{\partial y}{\partial \tau_s} = \alpha \frac{\partial^2 y}{\partial \rho^2} \quad (\text{surface diffusion}). \quad (7)$$

The initial and boundary conditions (I.C. and B.C.) are given by Eq. (8):

$$\left. \begin{array}{l} \text{(I.C.) } y = 0 \quad \text{at } \tau_p = 0 \text{ or } \tau_s = 0 \\ \text{(B.C.) } y = 1 \quad \text{at } \rho = 0 \quad \partial y / \partial \rho = 0 \text{ at } \rho = 1 \end{array} \right\} \quad (8)$$

Equations (6) and (7) were transformed into finite difference equations and solved numerically.

## Results and discussion

Figure 2 shows the equilibrium isotherms for adsorption of a) C.I. Acid Red 18 (AR18) and b) C.I. Acid Red 27 (AR27) onto the cellulose membrane in the presence of different concentration of sodium chloride ( $C_E$ ). Sodium chloride was added to stimulate dye adsorption. These dyes required high concentration of sodium chloride for adsorption because of high density of electric charge. The amount of equilibrium adsorption,  $q'_0$  (mol/kg) of AR27 is twice that of AR18 in the presence of the same concentration of sodium chloride, because the presence of 8-sulfonate group of AR18 prevents dye-cellulose interaction (association) as well as dye-dye self-association (aggregation) [12]. Tables 1 and 2 summarize the experimental Freundlich constants ( $k$  and  $\gamma$  of  $q = kC^\gamma$ ), which were determined from the intercepts and slopes of each lines in Fig. 2. Though the values of  $k$  depend on the concentration of NaCl, they correlate with the affinity of the dyes onto the substrate. The magnitude of  $k$  of AR18 at  $C_E = 2$  mol/dm<sup>3</sup> is nearly equal to that of AR27 at  $C_E = 0.5$

mol/dm<sup>3</sup>. The values of  $\alpha$  in Eq. (2) of each run were also summarized in Tables 1 and 2.

As the amount of equilibrium adsorption of these dyes was very low, the kinetic experiments were carried out at  $C_E$  in Tables 1 and 2. Figure 3 shows the experimental uptake curves of AR18 measured by using one sheet of cellulose membrane.  $[A']$  represents mean concentration of dye in membrane [7]. The bulk phase concentration of NaCl ( $C_E$ ) is 2 mol/dm<sup>3</sup>. The amount of the dye adsorbed onto the substrate depends on dye concentration in the bulk solution ( $C_0$ ). The solid and broken lines show the theoretical lines for surface diffusion control (Eq. (7)) and pore diffusion control (Eq. (6),  $\beta = 0$ ), respectively. The experimental data can be correlated well by both models. The surface diffusivity based on surface diffusion control,  $D'_s$  (m<sup>2</sup>/s) and pore diffusivity based on pore diffusion control,  $D'_p$  (m<sup>2</sup>/s) were determined by matching the theoretical values calculated from Eqs. (7) and (6) with the data, respectively (see Tables 1 and 2).

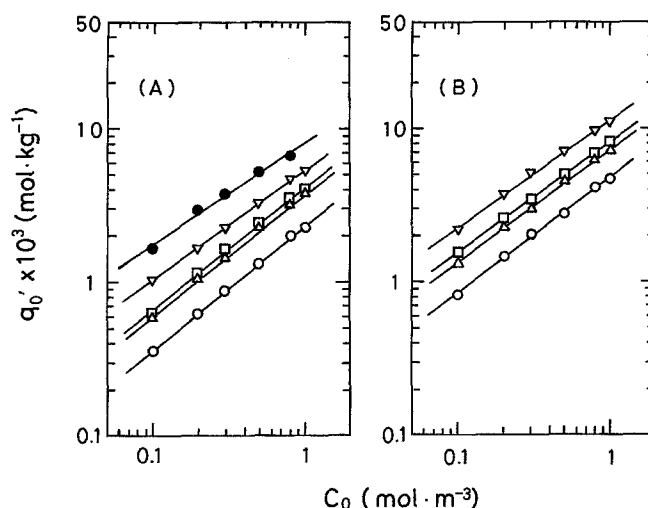


Fig. 2 Adsorption isotherms of (A) C.I. Acid Red 18 and (B) C.I. Acid Red 27 on a cellulose membrane in the presence of various concentrations of NaCl ( $C_E$ ) at 25°C.  $C_E$  = ○:0.1, △:0.3, □:0.5, ▽:1.0, ●:2.0 mol/dm<sup>3</sup>

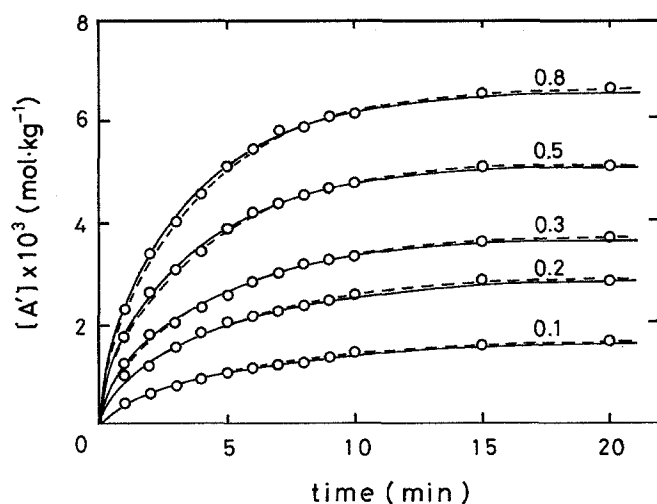
Table 1 Physical properties in the cellulose membrane – C.I. Acid Red 18 system at 25°C

Run No <sup>a</sup>	$C_0$ mol/m <sup>3</sup>	$C_E$ mol/dm <sup>3</sup>	$\alpha$	$k$	$\gamma$	$D'_s \times 10^{12}$ m <sup>2</sup> /s	$D'_p \times 10^{12}$ m <sup>2</sup> /s
1 (1)	0.10	1.00	5.96	2.24	0.721	1.66	8.63
2 (1)	0.20	1.00	4.64	2.24	0.721	2.25	8.71
3 (1)	0.10	2.00	9.46	3.40	0.666	1.93	15.6
4 (1)	0.20	2.00	8.35	3.40	0.666	2.18	15.2
5 (1)	0.30	2.00	7.16	3.40	0.666	2.53	14.3
6 (1, 10)	0.50	2.00	6.00	3.40	0.666	2.94	13.7
7 (1, 10)	0.80	2.00	4.75	3.40	0.666	3.37	12.2

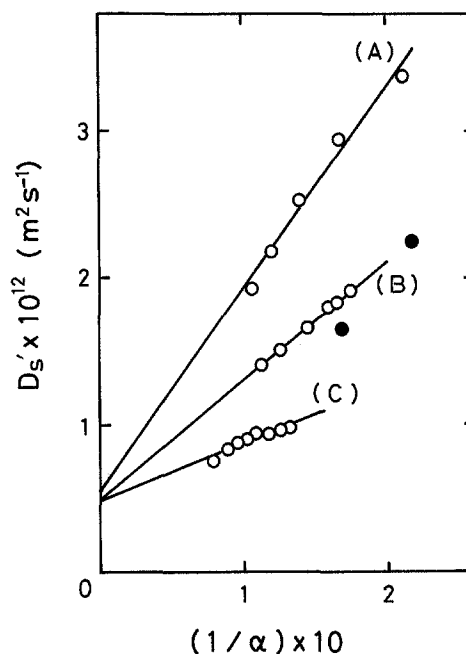
<sup>a</sup> The numbers in the parentheses shows the number of sheets of the membrane superposed.

**Table 2** Physical properties in the cellulose membrane – C.I. Acid Red 27 system at 25 °C

Run No <sup>a</sup>	$C_0$ mol/m <sup>3</sup>	$C_E$ mol/dm <sup>3</sup>	$\alpha$	$k$	$\gamma$	$D'_s \times 10^{13}$ m <sup>2</sup> /s	$D'_p \times 10^{12}$ m <sup>2</sup> /s
1 (1)	0.10	1.00	12.8	4.82	0.711	7.57	8.53
2 (1)	0.15	1.00	11.3	4.82	0.711	8.30	8.12
3 (1, 10)	0.20	1.00	10.5	4.82	0.711	8.78	7.88
4 (1)	0.25	1.00	9.81	4.82	0.711	9.05	7.59
5 (1)	0.30	1.00	9.29	4.82	0.711	9.41	7.52
6 (1)	0.40	1.00	8.56	4.82	0.711	9.39	6.87
7 (1)	0.50	1.00	8.03	4.82	0.711	9.62	6.75
8 (1)	0.60	1.00	7.60	4.82	0.711	9.81	6.45
9 (1)	0.10	0.50	8.88	3.45	0.725	14.1	10.5
10 (1)	0.15	0.50	7.95	3.45	0.725	15.1	9.86
11 (1)	0.25	0.50	6.90	3.45	0.725	16.6	9.47
12 (10)	0.30	0.50	6.57	3.45	0.725	—	—
13 (1)	0.35	0.50	6.29	3.45	0.725	18.0	9.32
14 (1)	0.40	0.50	6.06	3.45	0.725	18.3	9.10
15 (1)	0.50	0.50	5.71	3.45	0.725	19.1	9.04

<sup>a</sup> The numbers in the parentheses shows the number of sheets of the membrane superposed.**Fig. 3** Effects of dye concentration ( $C_0$ ) on uptake curves of C.I. Acid Red 18 at 25 °C ( $C_E = 2$  mol/dm<sup>3</sup>). Numbers on the lines represent  $C_0$  (mol/m<sup>3</sup>). (—): theoretical line for surface diffusion control (Eq. (7)), (---): theoretical line for pore diffusion control (Eq. (6))

As described in our previous paper [10], the surface diffusivity of the parallel diffusion model ( $D'_s$ ) can be obtained by plotting  $D'_s$  versus  $1/\alpha$ , then it was represented in Fig. 4. The plots of AR18 at  $C_E = 2$  mol/dm<sup>3</sup> were correlated by a line, although those of at  $C_E = 1$  mol/dm<sup>3</sup> deviated from the line. This will be because AR18 has not enough affinity at  $C_E = 1$  mol/dm<sup>3</sup>. On the other hand, the plots of AR27 were correlated by two lines depending on NaCl concentration, which have almost the same intercepts and different slopes. As mentioned in our previous paper [10], the increase of  $D'_s$  with increasing  $1/\alpha$  indicates the increasing contribution of pore diffusion with

**Fig. 4** The relation between the surface diffusivity based on surface diffusion control ( $D'_s$ ) and  $1/\alpha$  at 25 °C. (A) AR18,  $C_E = 2$  mol/dm<sup>3</sup>, (B) AR27,  $C_E = 0.5$  mol/dm<sup>3</sup>, (C) AR27,  $C_E = 1$  mol/dm<sup>3</sup>. ● represents AR18 at  $C_E = 1$  mol/dm<sup>3</sup>

decreasing  $\alpha$ . The surface diffusivity for the parallel diffusion model  $D'_s$  could be obtained from the intercepts of the lines.

Figure 5 shows the effects of  $\alpha$  on  $D'_p$  which was determined by assuming pore diffusion control (see Fig. 3). It appears that the plots for AR18 at  $C_E = 2$  mol/dm<sup>3</sup> were correlated by a line. On the other hand, the experimental

values of  $D'_p$  for AR27 are correlated well by two straight lines depending on NaCl concentration, which have different intercepts and nearly the same slopes. As mentioned in our previous paper [8], the increase of  $D'_p$  with increasing  $\alpha$  indicates an increasing contribution of surface diffusion. The pore diffusivity for the parallel diffusion model  $D_p$  was obtained from the intercepts of the lines [8]. The reason the plots of AR27 are represented by two lines is because we suppose that dye molecules of AR27 exist in different forms in the solution, depending on NaCl concentration.

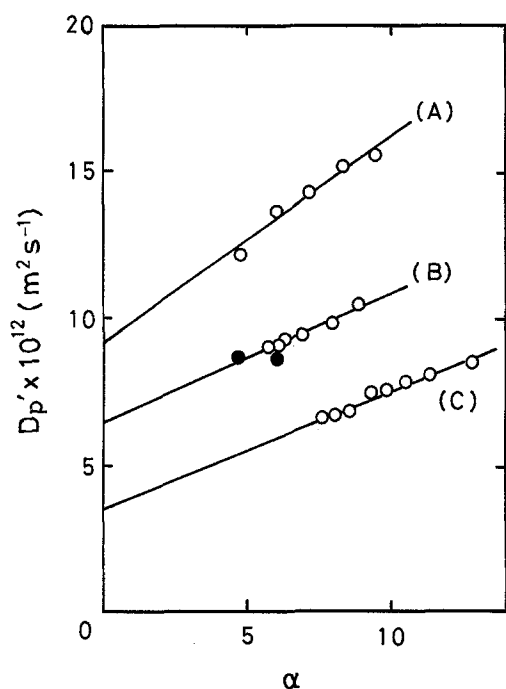


**Fig. 5** Effects of  $\alpha$  on the pore diffusivity based on pore diffusion control ( $D'_p$ ) at 25°C. (A) AR18,  $C_E = 2 \text{ mol/dm}^3$ , (B) AR27,  $C_E = 0.5 \text{ mol/dm}^3$ , (C) AR27,  $C_E = 1 \text{ mol/dm}^3$ . ● represents AR18 at  $C_E = 1 \text{ mol/dm}^3$

A part of dye molecules of AR27 must form a dimer in the liquid phase at  $C_E = 1 \text{ mol/dm}^3$ , although the aggregation constant of the dye is very low due to three sulfonate groups [12,13]. And it hardly aggregates at  $C_E = 0.5 \text{ mol/dm}^3$ . The values of  $D_s$  and  $D_p$  obtained from Figs. 4 and 5 were summarized in Table 3.

Figure 6 shows the concentration-distance profiles of AR18 and AR27 obtained by placing a stack of 10 membranes together during uptake and separating them for concentration analysis. The lines in the figure represent the theoretical lines for the parallel diffusion model calculated using  $D_s$  and  $D_p$  in Table 3 and Eq. (6). The theoretical lines agree fairly well with the experimental value, although slight disagreement was observed at both ends of a stack of membrane for the profile of AR27 at  $C_E = 1.0 \text{ mol/dm}^3$ ,

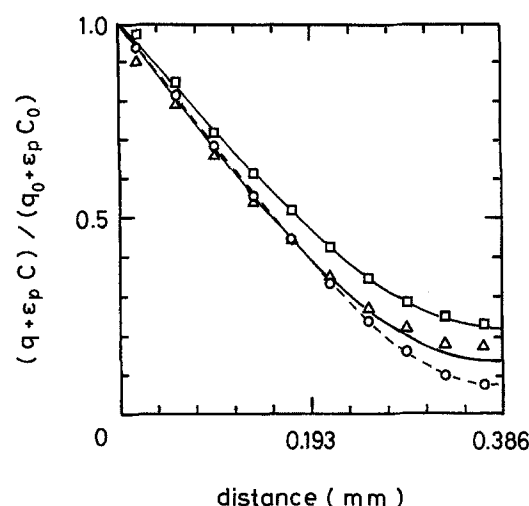


**Fig. 6** The concentration-distance profiles in the stacked membrane at 25°C. The solid and broken lines in the figure represent the theoretical lines for parallel diffusion calculated using  $D_s$  and  $D_p$  in Table 3. ○: Run 6 in Table 1, 3 h,  $\beta = 0.356$ , □: Run 12 in Table 2, 6 h,  $\beta = 0.523$ , △: Run 3 in Table 2, 8 h,  $\beta = 1.53$

**Table 3** Physical properties of various dyes in the cellulose membrane at 25°C

Dye (C.I. No.) (code)	M.W.	valency	$C_E$ mol/m <sup>3</sup>	$\alpha$	$k$	$D_s \times 10^{14}$ m <sup>2</sup> /s	$D_p \times 10^{13}$ m <sup>2</sup> /s	$\beta$
Direct Yellow 12 <sup>7)</sup> (DY12)	680.7	2	20–30	26.0–181	15.9–25.4	1.52	3.00	1.32–9.18
Direct Yellow 4 <sup>15)</sup> (DY4)	624.2	2	20–50	25.7–62.5	13.3–22.1	2.37	6.12	0.995–2.42
Acid Red 18 (AR18)	604.5	3	2000	4.75–9.46	3.46	54.3	91.4	0.282–0.562
Acid Red 27 (AR27)	604.5	3	500 1000	5.71–8.88 7.60–12.8	3.45 4.82	49.1 48.4	64.5 35.3	0.454–0.706 1.04–1.75
Acid Blue 40 <sup>15)</sup> (AB40)	473.4	1	30–50	10.2–16.3	4.35–5.67	37.9	9.41	4.11–6.57
Acid Red 88 <sup>9)</sup> (AR88)	400.4	1	10–30	2.63–22.7	1.93–5.17	36.4	1.97	4.84–41.8

which may be caused by the presence of a small amount of dimer. Therefore, we concluded that diffusion of these dyes could be described by the parallel diffusion model.

As mentioned in our previous paper [9], a linear relationship was observed between the logarithmic plots of the surface diffusivity ( $D_s$ ) and molecular weight of dyes at 55 °C. Accordingly, the same plots were attempted at 25 °C. Diffusivities and molecular weight of C.I. Direct Yellow 12 (7) and C.I. Direct Yellow 4 (15), C.I. Acid Blue 40 (15) and C.I. Acid Red 88 (9) shown in Fig. 1 were summarized in Table 3 and plotted in Fig. 7. A linear relationship was observed between  $D_s$  and molecular weight for C.I. Direct Yellow 12 (DY12), C.I. Direct Yellow 4 (DY4) and C.I. Acid Red 88 (AR88), however, those of AR27, AR18 and C.I. Acid Blue 40 (AB40) deviated apart from the line. The reason was assumed that the affinities of AR27, AR18 and AB40 were smaller than the values expected on the basis of their molecular weight due to three sulfonate groups of AR18 and AR27 and nonlinearity of the structure of AB40. Then, we tried to plot  $D_s$  versus Freundlich constant,  $k$  as a measure of an affinity in Fig. 8. By the way,  $D_s$  and  $D_p$  for DY12, DY4, AB40 and AR88 were obtained by the experiments at different NaCl concentration. As the values of  $k$  depend on NaCl concentration as shown in Table 3, a larger value of  $k$  was used to represent the affinity of the dyes. Then, good correlation was observed between  $D_s$  and  $k$ . On the other hand, there is no correlation between  $D_p$  and molecular weight (or  $k$ ).

Fig. 7 Relation between the surface diffusivity for the parallel diffusion model ( $D_s$ ) at 25 °C and molecular weight of the dyes

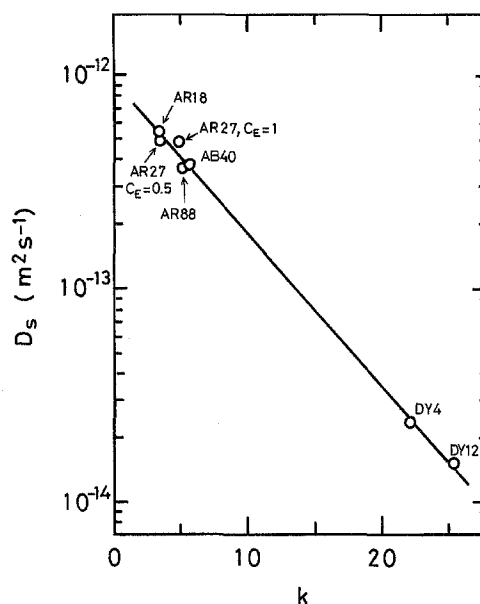
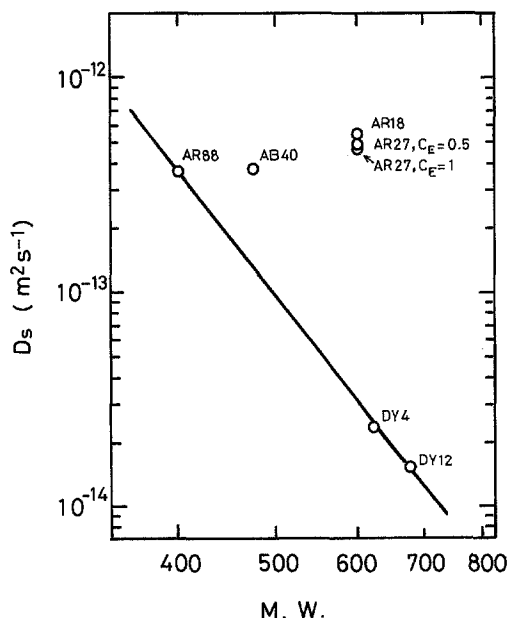


Fig. 8 Relation between the surface diffusivity for the parallel diffusion model ( $D_s$ ) and Freundlich constant  $k$  as a measure of an affinity at 25 °C

The magnitude of  $D_p$  seemed to be affected complicatedly by the condition of the dye in the liquid phase like aggregation.

The value of  $\beta$  ( $= \alpha D_s / D_p$ ) is an indicator of the type of controlling diffusion. Diffusion is controlled by surface diffusion for  $\beta > 10$ , and by pore diffusion for  $\beta < 0.1$ . Parallel diffusion occurs for  $0.1 \leq \beta \leq 10$  (5). Accordingly, all dyes except AR88 in Table 3 diffuse parallelly at 25 °C. The smaller values of  $\beta$  for AR18 at  $C_E = 2$  mol/dm³ and AR27 at  $C_E = 0.5$  mol/dm³ indicate the larger contribution of pore diffusion in parallel diffusion.

## Conclusions

Adsorption and diffusion of tri-sulfonated monoazo dyes into a cellulose membrane were analyzed on the basis of a parallel diffusion model. The following conclusions were made. The diffusion of the dyes with a low affinity could be described by the model provided that adsorption was stimulated by addition of high concentration of sodium chloride. The surface diffusivity for the parallel diffusion model was correlated by an affinity of the dyes. On the other hand, the pore diffusivity for the model was affected by aggregation of dye molecules in the liquid phase depending on its structure and NaCl concentration.

## References

1. McGreger R, Peters RH, Petropoulos JH (1962) *Trans Faraday Soc* 58: 1045
2. Warwicker JO (1963) *J Polym Sci Part A* 1:3105
3. Hori T, Mizuno M, Shimizu T (1980) *Colloid Polym Sci* 258:1070
4. Morita Z, Tanaka T, Motomura H (1986) *J Appl Polym Sci* 31:777
5. Yoshida H, Kataoka T, Nango M, Ohta S, Kuroki N, Maekawa M (1986) *J Appl Polym Sci* 32:4185
6. Yoshida H, Kataoka T, Maekawa M, Nango M (1989) *Chemical Eng J* 41:B1
7. Yoshida H, Maekawa M, Nango M (1991) *Chemical Eng Sci* 46:429
8. Maekawa M, Murakami K, Yoshida H (1993) *J Colloid Interface Sci* 155:79
9. Maekawa M, Tanaka M, Yoshida H (1995) *J Colloid Interface Sci* 170:146
10. Maekawa M, Murakami K, Yoshida H (1995) *Colloid Polym Sci* 273:793
11. Robinson C, Mills H (1931) *Proc R Soc London A* 131:576
12. Zollinger H, Back G, Milicevic B, Roseria AN (1961) *Melliand Textiltech* 42:73
13. Hamada K, Nonogaki H, Fukushima Y, Munkbat B, Mitsuishi M (1991) *Dyes Pigm* 16:111
14. Hamada K, Mitsuishi M (1992) *Dyes Pigm* 19:161
15. Unpublished data